Catalysis Today 183 (2012) 79–87

Contents lists available at SciVerse ScienceDirect

Catalysis Today

journal homepage: www.elsevier.com/locate/cattod

Effect of the zirconia addition manner on the modification of Fe–SiO_2 interaction

Ming Qing[a,b,c], Yong Yang[a,b,*], Baoshan Wu[a,b], Hong Wang[b], Hulin Wang[b], Jian Xu[b], Chenghua Zhang[a,b], Hongwei Xiang[a,b], Yongwang Li[a,b]

[a] State Key Laboratory of Coal Conversion, Institute of Coal Chemistry, Chinese Academy of Sciences, Taiyuan 030001, People's Republic of China
[b] National Engineering Laboratory for Indirect Coal Liquefaction, Institute of Coal Chemistry, Chinese Academy of Sciences, Taiyuan 030001, People's Republic of China
[c] Graduate School of the Chinese Academy of Sciences, Beijing 100039, People's Republic of China

ARTICLE INFO

Article history:
Received 25 June 2011
Received in revised form 27 October 2011
Accepted 27 October 2011
Available online 23 November 2011

Keywords:
Fischer–Tropsch synthesis
Fe–SiO_2 interaction
Zirconia modification
Preparation method
Fourier transform infrared spectroscopy

ABSTRACT

A series of ZrO_2-modified Fe/SiO_2 catalysts with the same composition were prepared by different methods. These solids were characterized by N_2 adsorption, Fourier transform infrared spectroscopy, temperature-programmed reduction, temperature-programmed desorption, transmission electronic microscopy and Mössbauer spectroscopy. The results indicated that the modification of Fe–SiO_2 interaction was strongly depended on the method of preparation. It was found that the strong Fe–SiO_2 interaction could be effectively weakened if Zr species and SiO_2 were pre-precipitated (Zr2-B and Zr2-C catalysts), even though the ZrO_2 level was low. Consequently, the reduction and carburization ability of the catalyst was enhanced and the Fischer–Tropsch synthesis activity was increased eventually. The products selectivity variation trend indicated that the selectivity to gaseous and light hydrocarbons was increased, whereas that to heavy hydrocarbons and olefin was suppressed when the Zr species and SiO_2 were precipitated before the precipitation of Fe^{3+} cation.

1. Introduction

The ever-increasing shortage of crude oil reserves has aroused renewed interest in alternative liquid fuels for the future and increasingly stringent environmental regulations push the drive for clean-fuels (low-sulfur, low-aromatics). Fischer–Tropsch synthesis (FTS), an environmental-friendly and economically promising route for the production of middle distillate fuels, petroleum blending-stock, and a wide variety of hydrocarbons and oxygenates from either coal or natural gas or biomass-derived syngas, has been paid great attention by numerous governments and academic institutions in recent years [1,2]. The lower price, moderate water gas shift (WGS) reaction activity and broad operation conditions of iron-based catalysts make them the most attractive catalysts for the industrial application [3,4]. Despite of this, the pure iron catalysts are not suitable for large-scale commercial applications. Promoters are commonly needed to improve the performance of iron catalysts. For example, Cu is added to facilitate the reduction of iron oxides [5,6] and K is usually employed to increase the heavy hydrocarbons content in the products [7,8]. Besides, SiO_2 is one of the most frequently employed support or binder in iron-based FTS catalysts [9–11]. The incorporation of SiO_2 enhanced the stability of iron catalysts, while this paid a penalty in catalyst activity simultaneously. These effects of SiO_2 were ascribed to the so-called Fe–SiO_2 interaction by many researchers for years, although the nature of this interaction was still in dispute [10–12].

In our previous study [13], the details of the Fe–SiO_2 interaction was scrutinized. The results showed that the Fe–SiO_2 interaction could be well explained in terms of the formation Fe–O–Si structure between iron oxides and SiO_2, and this structure was formed during the dehydration process. The physico-chemical properties and FTS reaction behaviors of the SiO_2-containing catalysts were well correlated with the influence of Fe–O–Si structure. Also, a series of Fe/SiO_2 catalysts promoted by different amounts of ZrO_2 were prepared (namely Zr1, Zr2, Zr5, Zr10, Zr20 and Zr40), then the promotional effect of ZrO_2 was thoroughly studied. It was found that the strong Fe–SiO_2 interaction could be effectively weakened by proper amount of ZrO_2 via disturbing the Fe–O–Si structure. As a result, the reduction and carburization ability was enhanced, and the FTS reaction performance was improved eventually. However, this modification effect of ZrO_2 cannot be observed when its content was relatively low (for catalyst Zr1, Zr2 and Zr5). It was generally accepted that the structures and properties of the catalysts varied with their preparation methods, even though their compositions were fixed [14]. Feller et al. [15] found that the ZrO_2 addition manner played a significant role in determining the properties of ZrO_2-promoted Co/SiO_2 catalysts.

* Corresponding author at: State Key Laboratory of Coal Conversion, Institute of Coal Chemistry, Chinese Academy of Sciences, Taiyuan 030001, People's Republic of China. Tel.: +86 351 7560835; fax: +86 351 7560835.
E-mail address: yyong@sxicc.ac.cn (Y. Yang).

0920-5861/$ – see front matter © 2011 Published by Elsevier B.V.
doi:10.1016/j.cattod.2011.10.024

The present study aims to investigate the effect of preparation method on the modification of Fe–SiO_2 interaction, to check whether the strong Fe–SiO_2 interaction could be weakened by ZrO_2 or not if proper manner was employed to prepare the catalysts, even though the ZrO_2 content was relatively low. Note that we did not examine the effect of ZrO_2 content variation on the modification of Fe–SiO_2 interaction in this study, since it has been scrutinized previously. A series of ZrO_2-promoted Fe/SiO_2 catalysts with the same composition were prepared by three different methods. The catalysts were characterized by N_2 adsorption, Fourier transform infrared spectroscopy (FTIR), H_2 temperature-programmed reduction (H_2-TPR), H_2 temperature-programmed desorption (H_2-TPD), transmission electronic microscopy (TEM) and Mössbauer effect spectroscopy (MES). The FTS performance of catalysts was tested in a fixed-bed reactor and correlated with the characterization results.

2. Experimental

2.1. Catalyst preparation

The catalyst precursors used in present study were prepared by coprecipitation method. A solution containing $Fe(NO_3)_3$ (99.9+%; Tianjin Chemical Co., P.R. China), and/or silica sol (SiO_2, 30.0 wt%; Qingdao Ocean Chemical Co., P.R. China) with an Fe/SiO_2 weight ratio of 100/20 was mixed and then introduced into a 5 L precipitation vessel at 80 ± 1 °C. A NH_4OH solution (Tianjin Chemical Co.) was added simultaneously into this precipitation vessel to maintain the pH at a constant value of 8.5 ± 0.3. The obtained precipitate was completely washed with hot deionized water, and then filtered. After that, the catalyst precursors were dried at 120 °C for 12 h, followed by calcined at 500 °C for 5 h in air. The obtained catalysts were denoted as FeSi. To examine the effect of preparation method on the modification of Fe–SiO_2 interaction, three ZrO_2-modified FeSi catalysts with the same composition (100Fe/20SiO_2/2ZrO_2) were prepared by different methods as described below: The mixed solution of $Fe(NO_3)_3$ (99.9+%; Tianjin Chemical Co., P.R. China), zirconium nitrate, and silica sol (SiO_2, 30.0 wt%; Qingdao Ocean Chemical Co., P.R. China) were precipitated with NH_4OH solution (Tianjin Chemical Co.) simultaneously, the resulting precipitate were sequentially washed, filtered, dried and calcined (Zr2-A). The mixed solution of zirconium nitrate and silica sol (SiO_2, 30.0 wt%; Qingdao Ocean Chemical Co., P.R. China) was firstly precipitated with NH_4OH solution (Tianjin Chemical Co.) to form a gel, which was divided into two equal parts. One of them was then mixed with $Fe(NO_3)_3$ (99.9+%; Tianjin Chemical Co., P.R. China) solution, followed by precipitation with NH_4OH solution, the obtained precipitate were washed, filtered, dried and calcined (Zr2-B). The other part of the gel was dried and calcined. Then the formed solid was crushed and powdered, which was mixed with $Fe(NO_3)_3$ (99.9+%; Tianjin Chemical Co., P.R. China) solution, followed by precipitation with NH_4OH solution, the resulting precipitate was also washed, filtered, dried and calcined (Zr2-C). All the experimental details (precipitation, washing, filtering, drying and calcination condition) employed in preparing these three catalysts (Zr2-A, Zr2-B, Zr2-C) were same to that of FeSi catalyst. The detailed catalysts composition and nomenclature were summarized in Table 1.

2.2. Catalyst handling and samples prepared for characterization

The reduced catalyst samples used for Mössbauer characterization were prepared by reducing the fresh catalysts in a quartz tube with synthesis gas (H_2/CO = 2.0) at 280 °C, 1000 h^{-1} of GHSV and 0.1 MPa for 24 h. After reduction, the sample was coated by paraffin wax to prevent any oxidation.

2.3. Catalyst characterization

The textural properties of fresh catalysts were determined via N_2 physisorption at −196 °C, using a Micromeritics ASAP 2420 instrument. Each sample was degassed under vacuum at 90 °C for 1 h and 350 °C for 8 h prior to the measurement.

The high-resolution transmission electronic microscopy (HRTEM) was performed at a JEOL 2010 HRTEM (JEOL, Japan) using an accelerating voltage of 200 kV. The calcined catalysts were dispersed in ethanol and mounted on a carbon foil supported on a copper grid.

The Mössbauer spectra of catalyst samples were obtained on an MR-351 constant-acceleration Mössbauer spectrometer (FAST, Germany) at room temperature and/or 20 K, using a 25 m Ci ^{57}Co in Pd matrix. The spectrometer was operated in a symmetric constant acceleration mode. The spectra were collected over 512 channels in the mirror image format.

The IR spectra were recorded with a VERTEX 70 (Bruker) FT-IR spectrophotometer. Powdered samples were diluted with KBr and pressed into translucent disks at room temperature. All spectra were taken in the 4000–400 cm^{-1} range at a resolution of 4 cm^{-1}.

The H_2-TPR was carried out using a dynamic analyzer (Micromeritics, Model 2920). About 40 mg of catalyst was treated in 10% H_2/90% Ar (v/v) (flow rate of 50 mL/min) and the reduction temperature was increased from room temperature to 800 °C at a heating rate of 10 °C/min. The hydrogen consumption was calibrated using the H_2-TPR of CuO (Aldrich, 99.99+%) as the standard sample at the same conditions.

The H_2-TPD was used to measure the hydrogen adsorption and desorption on H_2-reduced catalysts. The catalyst sample (100 mg) was firstly reduced in pure H_2 at 400 °C for 16 h and cooled to 50 °C. Then, the reduced sample was purged with Ar until the baseline of H_2 signal leveled off. Finally, the sample was heated to 800 °C at a ramp of 10 °C/min.

2.4. FTS performance

The FTS performance of the catalysts was tested in a stainless steel fixed bed reactor with an inner diameter of 12 mm. 5 mL catalyst was loaded into the reactor for all the reaction tests. The remaining volume of the reactor tube was filled with quartz granules at the size range of 20–40 mesh. All the catalysts were activated with syngas (H_2/CO = 2.0) at 280 °C, 0.10 MPa and 1000 h^{-1} for 24 h. The reaction conditions were controlled at 270 °C, 1.5 MPa, 2000 h^{-1} and H_2/CO = 2.0. The detailed description of the reactor and product analysis system has been provided elsewhere [11].

3. Results and discussion

3.1. BET surface area

Table 1 gives the results of N_2 physisorption for the catalysts. Great higher BET surface area (222 m^2/g) was found for FeSi catalyst compared with that of α-Fe_2O_3. In the previous study, it was concluded that iron oxides interacted with SiO_2 via Fe–O–Si structure in the catalysts containing SiO_2. Due to the formation of this structure, the particle agglomeration to form large iron oxides particle was restrained which resulted in the high dispersion state of iron oxides. This was considered to be the origin of the strong dispersion effect of SiO_2 matrix [13]. The BET surface area of Zr2-A catalyst was almost identical to that of FeSi catalyst. However, for Zr2-B and Zr2-C catalysts, the BET surface areas were decreased (in comparison to FeSi catalyst), which was more obvious for Zr2-C catalyst. The above results implied that the dispersion state of iron

Table 1
The composition and textural properties of the zirconia-promoted FeSi catalysts as-prepared.

Catalysts	Catalyst composition (parts by weight)	BET surface area (m^2/g)[a]	Pore volume (cm^3/g)[a]	Average pore size (nm)[a]
α-Fe_2O_3	–	25	0.16	29.3
FeSi	100Fe/20SiO_2	222	0.53	7.8
Zr2-A	100Fe/20SiO_2–2ZrO_2	223	0.61	8.9
Zr2-B	100Fe/20SiO_2–2ZrO_2	211	0.42	7.7
Zr2-C	100Fe/20SiO_2–2ZrO_2	171	0.49	9.1

[a] Max error = ±5%.

oxides was influenced by the addition manner of ZrO_2, as discussed in detail later.

3.2. Modification of Fe–SiO_2 interaction

Fig. 1 illustrates the FTIR spectra of the catalysts as-prepared, and the typical frequency values and assignments are summarized in Table 2 [4,16]. The bands, assigned to the vibration modes of H_2O and CO_2, have not been discussed here. Comparing the FTIR spectrum of FeSi catalyst with that of α-Fe_2O_3 (Fig. 1a), a new peak at 1000 cm^{-1} can be observed, which was assigned to the Fe–O–Si vibration [16–19], indicating that the so-called Fe–SiO_2 interaction could be explained in terms of the formation of Fe–O–Si bond between iron oxides and SiO_2. This structure was supposed to be formed during the drying process, and the detailed mechanism has been examined elsewhere [13]. As mentioned in BET analysis, the formation of Fe–O–Si structure in FeSi catalyst resulted in the high dispersion state of iron oxides. Therefore, the characteristic stretching vibration bands centred at 470 and 539 cm^{-1} of Fe–O bond became broad and less intensive in FeSi catalyst [20,21].

Fig. 1b shows the FTIR spectra of ZrO_2-modified FeSi catalysts prepared by different methods. It is apparent that the position of the peak at 1000 cm^{-1} of Zr2-A catalyst was similar to that of FeSi catalyst, implying that introducing ZrO_2 via this manner has less or no obvious influence on the Fe–SiO_2 interaction. According to the previous study [13], in which a series of ZrO_2-modified FeSi catalysts with different ZrO_2 content were prepared using the same method employed in Zr2-A catalyst, the strong Fe–SiO_2 interaction could only be weakened by ZrO_2 when its content was high enough. For the Zr2-B catalyst, the band at 1000 cm^{-1} representing Fe–O–Si structure did not change significantly (relative to that of FeSi catalyst). However, it should be noted that a shoulder peak at 1113 cm^{-1} appeared, coinciding with the asymmetry stretching vibration of Si–O–Si, which suggested that part of SiO_2 did not interact with iron oxides in this sample. The Zr^{4+} and SiO_2 sol were precipitated before the precipitation of Fe^{3+} during the preparation process of Zr2-B catalyst, implying that the surface of silica was covered by a layer of zirconia species [22]. Consequently, part of sites on SiO_2 surface may not interact with iron species in the subsequent process, as evidenced in the spectrum of Zr2-B catalyst (the peak at 1113 cm^{-1}). The above results indicated that although the formed Fe–O–Si structure was not disturbed in Zr2-B catalyst, the amount of SiO_2 that interacted with iron oxides was reduced to some extent. In another word, the total strength of Fe–SiO_2 interaction was effectively weakened. Significant difference between the FTIR spectra of Zr2-C and FeSi catalysts can be discerned, as illustrated in Fig. 1b. It is obvious that the typical stretching vibration bands centred at 470 and 539 cm^{-1} of Fe–O bond in the FTIR spectrum became sharper and more intensive, indicating a relative higher crystallinity of iron oxides in this sample. Moreover, no obvious peak at 1000 cm^{-1} can be observed in the spectrum of Zr2-C catalyst, and the peak centre of the band shifted to 1113 cm^{-1}. These results suggested that most part of SiO_2 did not interact with iron oxides, thus almost no effective Fe–SiO_2 interaction formed in this sample. Let us review the preparation process of Zr2-C catalyst: the Zr^{4+} and SiO_2 sol were firstly precipitated and the obtained gel was then dried and calcined, during which the ZrO_2–SiO_2 interaction was strengthened. This means that the SiO_2 surface became inert after the pre-precipitation and thermal treatment mentioned above. Therefore, the formation of Fe–O–Si structure between iron oxides and SiO_2 was restrained during the subsequent process. Due to the absence of this structure, the dispersion effect of SiO_2 matrix was greatly reduced. As a result, large particles were formed caused by the iron oxides agglomeration during the thermal treatment, consistent with the BET analysis.

Table 2
IR frequencies (cm^{-1}) and assignment.

Frequencies (cm^{-1})	Assignment
3440	$\nu(H_2O)$
1624	$\delta(H_2O)$
2400	$\nu_{as}(CO_2)$
1113, 1070	ν_{as}(Si–O–Si) in solid state
803	ν_s(Si–O–Si)
474	δ(O–Si–O)
539	ν(Fe–O)
470	ν(Fe–O)

3.3. Reduction behavior of the catalysts

The reduction behaviors of the catalysts were measured by H_2-TPR. The reduction profiles and H_2 consumption for the catalysts are presented in Fig. 2 and Table 3, respectively. As can be seen, α-Fe_2O_3 catalyst exhibited the typical two-step reduction process of hematite, i.e., α-$Fe_2O_3 \rightarrow Fe_3O_4 \rightarrow \alpha$-Fe [10,23], which was verified by the amount of H_2 consumption (0.15 mol H_2/mol Fe for the lower temperature reduction peak and 1.28 mol H_2/mol Fe for the higher

Table 3
Quantitative results of H_2 consumption for the zirconia-promoted FeSi catalysts in H_2-TPR.[a,b]

Catalysts	Peak	Peak centre (°°C)	H_2 consumption (mol H_2/mol Fe)
α-Fe_2O_3	I	345	0.15
	II	508	0.52
	III	598	0.76
FeSi	I	373	0.47
	II	432	0.05
	III	608	0.60
Zr2-A	I	372	0.45
	II	433	0.04
	III	526	0.21
	IV	604	0.43
Zr2-B	I	370	0.40
	II	496	0.18
	III	593	0.62
Zr2-C	I	360	0.18
	II	563	0.72
	III	651	0.43

[a] The H_2 consumption was measured from the area under the corresponding peak.
[b] Max error = ±2%.

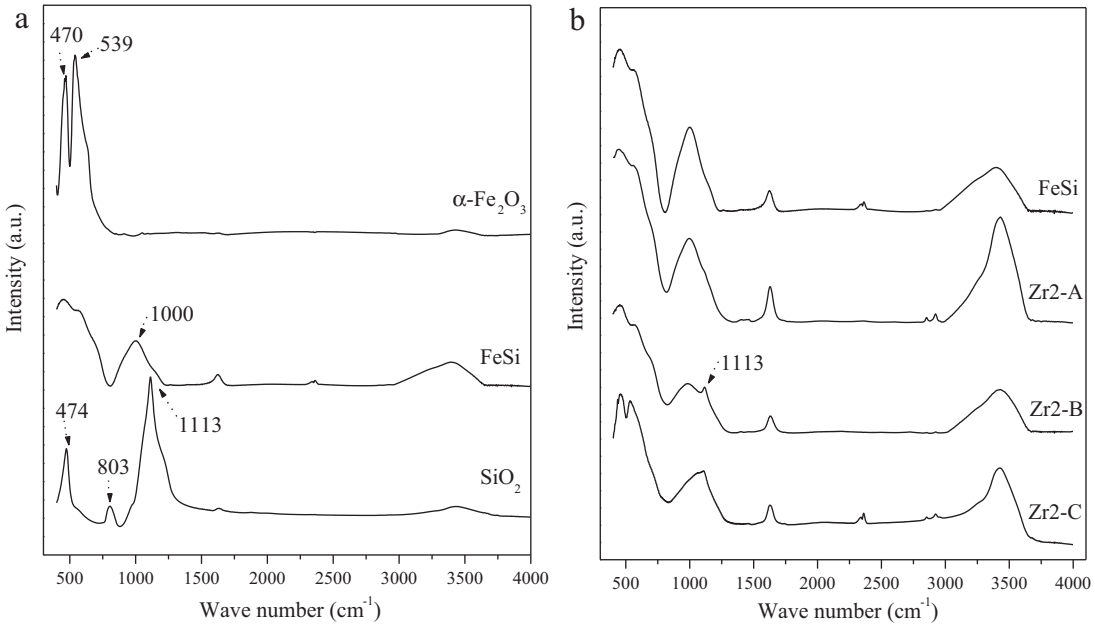

Fig. 1. FTIR spectra of the zirconia-promoted FeSi catalysts as-prepared.

one). However, FeSi catalyst exhibited two main broadened reduction regions. The onset of the first region was apparently retarded compared to that of α-Fe_2O_3, and this region was well fitted with two peaks (peaks I and II, see Supplementary Information, Fig. S1). Judging from the H_2 consumption, peak I should be ascribed to the reduction of α-Fe_2O_3 to Fe_3O_4 and part of Fe_3O_4 to Fe^{2+} species, and peak II may be composed of the reduction of the remainder Fe_3O_4 which strongly interacted with SiO_2 to Fe^{2+} species. The sum of H_2 consumption for peaks I and II (0.52 mol H_2/mol Fe), consistent with the theoretical value of Fe^{3+} to Fe^{2+} (0.5 mol H_2/mol Fe), verified the above statement. These Fe^{2+}/Si compounds can be present either in the form of wüstite (FeO) or Fe_2SiO_4, which cannot be reduced completely even at high temperature [10,12]. Thus, the total H_2 consumption (1.12 mol H_2/mol Fe) was significantly lower than that of theoretical α-Fe_2O_3 → α-Fe (1.5 mol H_2/mol Fe). It was concluded previously that iron oxides and SiO_2 interacted via Fe–O–Si structure, which lead to the partial electron transfer from Fe–O_{Fe} group to Si species. Therefore, the Fe–O_{Fe} bonds were strengthened and the removal of oxygen during reduction or activation became difficult (detailed discussion can be found elsewhere [13]).

It is generally accepted that Fe–SiO_2 interaction played a critical role in determining the reduction behavior of the catalysts containing SiO_2 [11–13,24–26]. Based on the reduction profiles illustrated in Fig. 2 and H_2 consumption listed in Table 3, one can find that the reduction behavior of Zr2-A catalyst was similar to that of FeSi catalyst. This was acceptable since the Fe–SiO_2 interaction was not modified by ZrO_2 in Zr2-A catalyst. For Zr2-B catalyst, the reduction behavior was changed. The H_2 consumption of the first reduction region (0.40 mol H_2/mol Fe) was reduced while the total value increased slightly (1.20 mol H_2/mol Fe) compared to that of FeSi catalyst. As confirmed by FTIR, part of SiO_2 did not interact with iron oxides, thus the total Fe–SiO_2 interaction strength was reduced. According to the studies reported before [10,12], Fe^{2+} species (FeO or Fe_2SiO_4) can only be stabilized where Fe–SiO_2 interaction is strong. Consequently, not all the α-Fe_2O_3 particles were reduced to Fe^{2+} species during the first reduction process due to the weakened Fe–SiO_2 interaction, which resulted in the reduced H_2 consumption. Moreover, the total reduction degree of iron oxides was enhanced in this catalyst. Significant difference of the reduction profile of Zr2-C catalyst was found in Fig. 2. Specifically, the first reduction peak shifted to lower temperature and it can be assigned to the reduction of α-Fe_2O_3 to Fe_3O_4 based on the H_2 consumption (0.18 mol H_2/mol Fe). Meanwhile, the total H_2 consumption was greatly increased (1.33 mol H_2/mol Fe). The FTIR results proved that almost no obvious Fe–O–Si structure formed in Zr2-C catalyst, indicating that the interaction between iron oxides and SiO_2 was neglectable to some extent in this sample. As a result, the iron oxide was reduced to Fe_3O_4 during the first reduction process and the total reduction degree increased greatly. The results discussed above indicated that the strong Fe–SiO_2 interaction could be effectively weakened by ZrO_2 if proper method was employed to prepare the catalysts, even though the ZrO_2 content was not high enough.

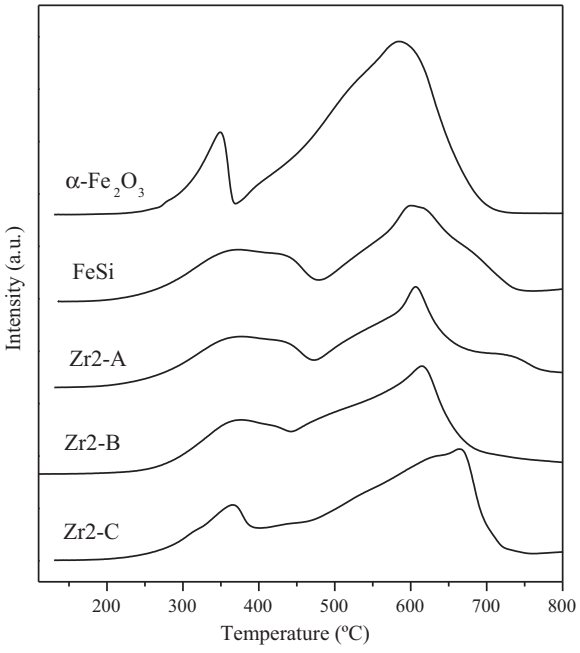

Fig. 2. H_2-TPR profiles of the zirconia-promoted FeSi catalysts.

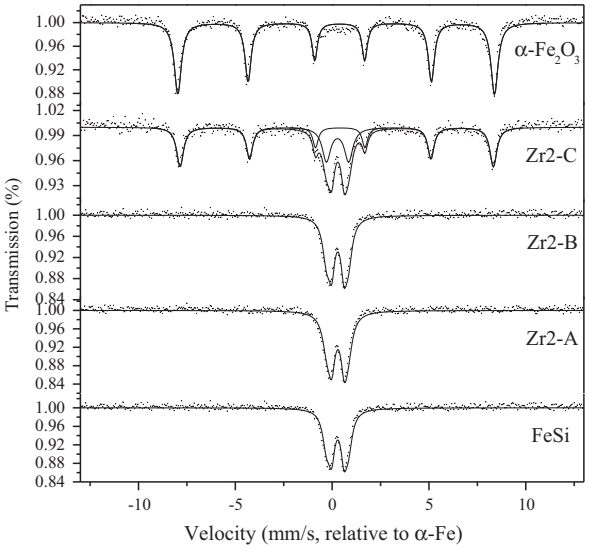

Fig. 3. Mössbauer spectra of the zirconia-promoted FeSi catalysts as-prepared measured at room temperature.

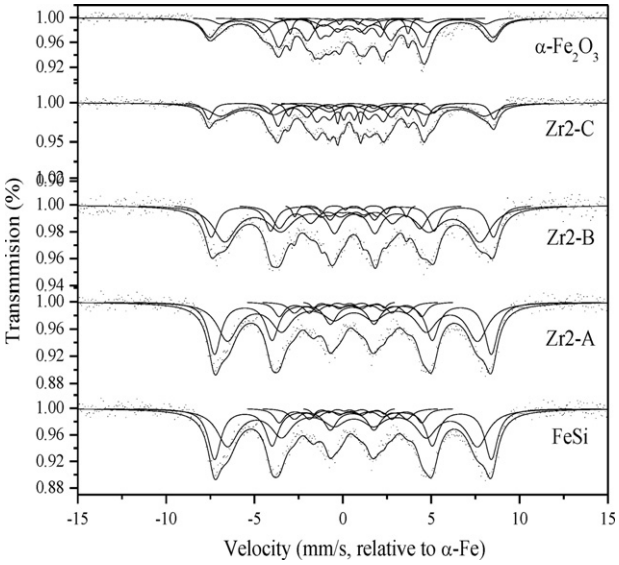

Fig. 4. Mössbauer spectra of the zirconia-promoted FeSi catalysts after reduction measured at 20 K.

3.4. Crystalline structure of the catalysts

Due to the highly dispersed properties of the iron oxides caused by the strong dispersion effect of SiO_2 [10,11], MES measured at room-temperature cannot give the detailed phase composition (see Supplementary Information, Tables S1 and S2). Thus, the crystalline structures of the reduced and used samples were measured by MES at 20 K.

3.4.1. Catalysts samples as-prepared

Fig. 3 illustrates the Mössbauer spectra of the fresh catalysts recorded at room temperature. The spectra parameters are given in Table 4. The α-Fe_2O_3 catalyst showed one sextet, which can be assigned to the (weak) ferromagnetic α-Fe_2O_3 with particle size larger than 13.5 nm [8,27–30]. For FeSi catalyst, the sextet disappears, and only the doublet was present. The Mössbauer parameters of the doublets were typical of superparamagnetic Fe^{3+} irons on the non-cubic sites with the crystallite diameters smaller than 13.5 nm [29–34]. The Mössbauer spectra of Zr2-A and Zr2-B catalysts were similar to that of FeSi catalyst, while the spectrum of Zr2-C catalyst was fitted by a combination of sextet and doublet. These results indicated that the particle size of SiO_2-containing catalysts was smaller than that of α-Fe_2O_3, and the particle size varied obviously with the preparation method of the catalysts. The HRTEM study was conducted to measure the particle size more accurately (see Supplementary Information, Figs. S2 and S3). One can find that the average particle size of FeSi catalyst (6 nm) was much smaller than that of α-Fe_2O_3 (33 nm), resulting from the strong dispersion effect of SiO_2. The evidence shown by FTIR indicated that the Fe–SiO_2 interaction was almost undisturbed by ZrO_2 in Zr2-A catalyst, while this interaction was weakened in Zr2-B catalyst. Moreover, no obvious Fe–SiO_2 interaction was formed in Zr2-C catalyst. As a result, the average particle size of Zr2-A was similar to that of FeSi catalyst, whereas those of Zr2-B (10 nm) and Zr2-C catalysts (20 nm) were increased (more significant for the latter).

3.4.2. Catalysts samples after reduction

Fig. 4 presents the Mössbauer spectra of the reduced catalysts measured at 20 K. The Mössbauer parameters and phase compositions are summarized in Table 5. All the Mössbauer patterns can be fitted with five sextets, representing Fe_3O_4 and iron carbides with different hyperfine parameters [35,36]. As can be seen, the reduction and carburization ability of FeSi catalyst was greatly restrained (lower χ-Fe_5C_2 content) compared to that of α-Fe_2O_3, ascribing to the strong Fe–SiO_2 interaction [13]. As for Zr2-A catalyst, the χ-Fe_5C_2 content was almost identical to that of FeSi catalyst. However, the weakened Fe–SiO_2 interaction resulted in the increased iron carbide content in the reduced Zr2-B catalyst, which was more obvious for Zr2-C catalyst.

3.4.3. Catalysts samples after FTS reaction

The catalysts after FTS reaction were also characterized by Mössbauer spectra at 20 K, as presented in Fig. 5. They can also be fitted with five sextets with different hyperfine parameters [35,36]. As summarized in Table 6, the used catalysts were composed of Fe_3O_4

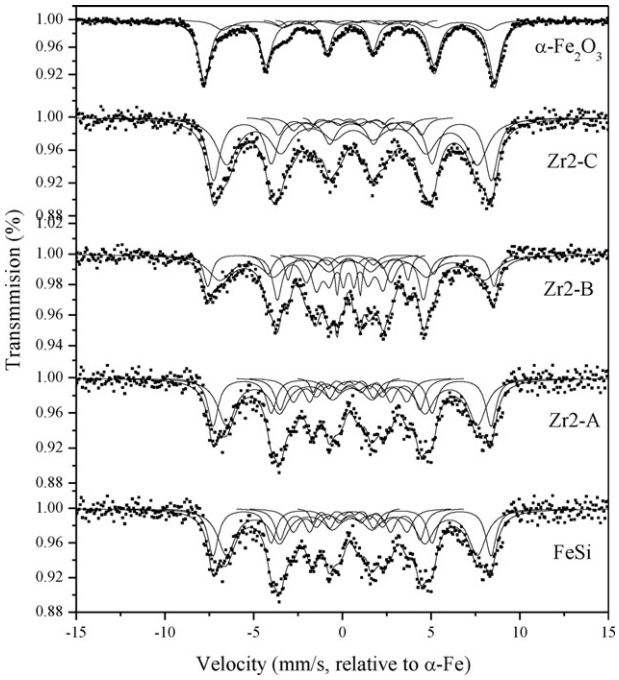

Fig. 5. Mössbauer spectra of the zirconia-promoted FeSi catalysts after FTS reaction measured at 20 K.

Table 4
Mössbauer parameters of the zirconia-promoted FeSi catalysts as-prepared obtained at room-temperature.

Catalysts	Phases	IS (mm/s)	QS (mm/s)	Hhf (kOe)	Area (%)[a]
FeSi	Fe^{3+} (spm)	0.36	0.86		100.0
Zr2-A	Fe^{3+} (spm)	0.31	0.85		100.0
Zr2-B	Fe^{3+} (spm)	0.30	0.88		100.0
Zr2-C	α-Fe_2O_3	0.30	−0.15	510	52.2
	Fe^{3+} (spm)	0.32	0.89		47.8
α-Fe_2O_3	α-Fe_2O_3	0.30	−0.15	513	100.0

[a] Max error = ±1%.

Table 5
Mössbauer parameters of the zirconia-promoted FeSi catalysts after reduction obtained at 20 K.[a,b]

Catalysts	IS (mm/s)	QS (mm/s)	Hhf (kOe)	Area (%)[c]	Assignment
FeSi	0.55	0.04	487	37.9	Fe_3O_4 (A)
	0.59	−0.08	440	44.9	Fe_3O_4 (B)
	0.43	0.00	251	8.4	χ-Fe_5C_2 (I)
	0.42	0.05	198	6.9	χ-Fe_5C_2 (II)
	0.37	−0.04	105	1.9	χ-Fe_5C_2 (III)
Zr2-A	0.55	−0.03	490	26.4	Fe_3O_4 (A)
	0.60	0.01	452	54.6	Fe_3O_4 (B)
	0.42	0.10	253	11.5	χ-Fe_5C_2 (I)
	0.41	0.10	207	5.0	χ-Fe_5C_2 (II)
	0.58	0.14	109	2.5	χ-Fe_5C_2 (III)
Zr2-B	0.53	−0.06	500	26.6	Fe_3O_4 (A)
	0.59	0.01	456	44.7	Fe_3O_4 (B)
	0.43	0.16	252	20.3	χ-Fe_5C_2 (I)
	0.34	0.29	200	2.2	χ-Fe_5C_2 (II)
	0.30	0.10	113	6.2	χ-Fe_5C_2 (III)
Zr2-C	0.54	0.00	500	18.0	Fe_3O_4 (A)
	0.60	−0.13	458	39.9	Fe_3O_4 (B)
	0.44	−0.10	251	23.5	χ-Fe_5C_2 (I)
	0.53	−0.20	199	9.7	χ-Fe_5C_2 (II)
	0.30	0.10	112	8.9	χ-Fe_5C_2 (III)
α-Fe_2O_3	0.55	−0.01	504	16.8	Fe_3O_4 (A)
	0.65	−0.01	459	32.8	Fe_3O_4 (B)
	0.45	0.09	252	20.5	χ-Fe_5C_2 (I)
	0.37	0.07	199	17.6	χ-Fe_5C_2 (II)
	0.36	0.13	109	12.3	χ-Fe_5C_2 (III)

[a] Reduction conditions: 280 °C, 0.1 MPa, H_2/CO = 2.0, 24 h and GHSV = 1000 h^{-1}.
[b] The data of Zr1 and Zr2 has been omitted since they are very similar to that of FeSi.
[c] Max error = ±1%.

Table 6
Mössbauer parameters of the zirconia-promoted FeSi catalysts after FTS reaction obtained at 20 K.[a,b]

Catalysts	IS (mm/s)	QS (mm/s)	Hhf (kOe)	Area (%)[c]	Assignment
FeSi	0.41	−0.05	485	33.2	Fe_3O_4 (A)
	0.64	0.09	439	33.8	Fe_3O_4 (B)
	0.47	0.14	245	16.6	χ-Fe_5C_2 (I)
	0.43	−0.02	200	11.8	χ-Fe_5C_2 (II)
	0.35	−0.12	112	4.7	χ-Fe_5C_2 (III)
Zr2-A	0.38	0.18	497	31.0	Fe_3O_4 (A)
	0.66	0.10	440	33.8	Fe_3O_4 (B)
	0.35	0.11	254	17.8	χ-Fe_5C_2 (I)
	0.30	−0.04	205	12.4	χ-Fe_5C_2 (II)
	0.30	0.10	109	5.0	χ-Fe_5C_2 (III)
Zr2-B	0.31	0.25	503	22.9	Fe_3O_4 (A)
	0.60	0.10	465	31.7	Fe_3O_4 (B)
	0.44	0.12	252	23.5	χ-Fe_5C_2 (I)
	0.40	0.01	205	12.4	χ-Fe_5C_2 (II)
	0.40	0.10	107	9.5	χ-Fe_5C_2 (III)
Zr2-C	0.48	0.00	502	32.0	Fe_3O_4 (A)
	0.59	0.12	464	45.8	Fe_3O_4 (B)
	0.41	0.10	256	12.3	χ-Fe_5C_2 (I)
	0.43	0.06	210	7.7	χ-Fe_5C_2 (II)
	0.38	0.06	112	2.2	χ-Fe_5C_2 (III)
α-Fe_2O_3	0.39	0.06	508	30.5	Fe_3O_4 (A)
	0.66	0.04	463	63.0	Fe_3O_4 (B)
	0.40	−0.10	251	3.5	χ-Fe_5C_2 (I)
	0.32	0.01	202	3.0	χ-Fe_5C_2 (II)

[a] Reaction conditions: 270 °C, 1.5 MPa, H_2/CO = 2.0 and GHSV = 2000 h^{-1}.
[b] The data of Zr1 and Zr2 has been omitted since they are very similar to that of FeSi.
[c] Max error = ±1%.

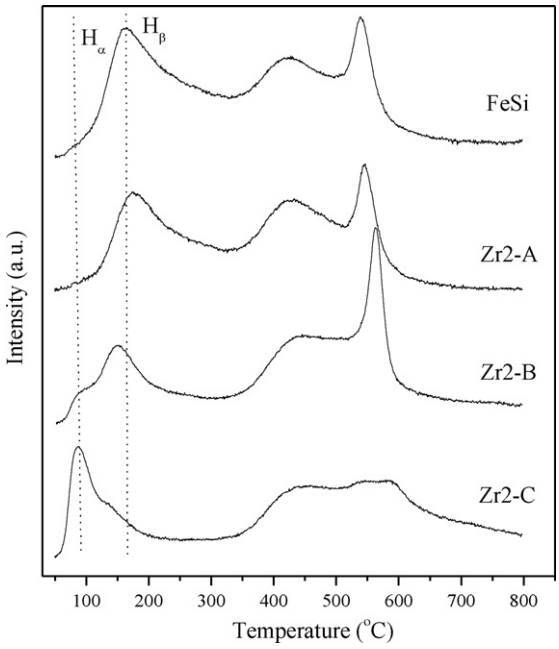

Fig. 6. H_2-TPD profiles of the zirconia-promoted FeSi catalysts.

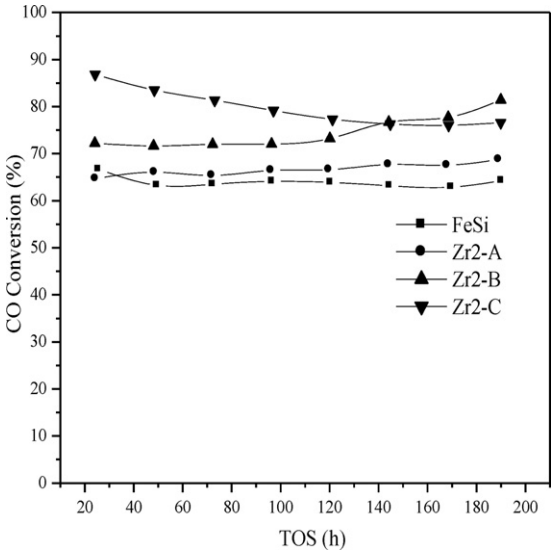

Fig. 7. CO conversion as a function of time on stream of the zirconia-promoted FeSi catalysts.

and χ-Fe_5C_2 with different ratios. For all the SiO_2-containing catalysts, the χ-Fe_5C_2 content in the used catalysts increased to a certain extent during FTS reaction due to the further carburization [11,13]. As for Zr2-C catalyst, however, the iron carbide content was decreased after the FTS reaction, implying that the χ-Fe_5C_2 was oxidized during reaction.

3.5. H_2 chemisorption

H_2-TPD was conducted to investigate the H_2 chemisorption behaviors of the catalysts, as illustrated in Fig. 6. It can be seen that the H_2 desorption could be assigned to several different adsorbed H species: desorbing around 100 °C (H_α), desorbing between 150 and 300 °C (H_β), and desorbing higher than 300 °C (H_γ) [37]. As reported in the literature [38], H_α represented the H species adsorbed on the surface metallic iron, and H_γ corresponded to the cleavage of OH species presented on the non reduced oxide surface in the catalysts. The higher desorption temperature of the H_γ species indicated that they were strongly adsorbed on the catalysts surface. It was expected that these species would not exert significant influence on the reaction behavior of the catalysts. The H_β could be tentatively assigned to the H species adsorbed on the sub-layer metallic iron tentatively, since no assignment of this species has been reported ever.

As shown in Fig. 6, almost no peak assigned to H_α was observed both in FeSi and Zr2-A catalysts, and the H_β desorption peak of Zr2-A catalyst shifted to higher temperature slightly (compared to that of FeSi catalyst), indicating that the H species adsorbed on this sample was more stable. However, for Zr2-B and Zr2-C catalysts, H_α desorption peak were observed, which was more obvious for the latter. It is apparent that the H_β desorption peak shifted to lower temperature for Zr2-B catalyst, while this species was absent on the Zr2-C catalyst surface. Judging from the desorption temperature of the H species adsorbed; it is reasonable that the H_α is more reactive than H_β. These results implied that the H_2 adsorption behavior was greatly influenced by introducing ZrO_2 into FeSi catalyst via different manners.

3.6. FTS performances

The FTS performances of the catalysts were measured at the reaction conditions of 270 °C, 1.5 MPa, $H_2/CO = 2.0$ and GHSV = 2000 h^{-1}. The activity, stability, and product selectivity were tested within a period of about 200 h steady-state runs. All the catalysts were tested under the same condition to examine the promotional effect of ZrO_2.

3.6.1. FTS performances of the catalysts

The effects of the preparation method on the FTS performances of ZrO_2-modified FeSi catalysts are presented in Fig. 7. The CO conversion was used as a measure of FTS activity in present study [11]. The results showed that the activity of Zr2-A catalyst kept almost unchanged during the entire reaction period, very similar to that of FeSi catalyst. It was found that the activity of Zr2-B catalyst increased slightly with time on stream (TOS). As for Zr2-C catalyst, the CO conversion decreased gradually although its initial activity was the highest among all the catalysts studied herein. Despite the on going discussion regarding the active species, a correlation between the carbide level of the catalyst and its activity in FTS has been observed by several authors [39–41]. Therefore, the iron carbides content determined by MES can be used to monitor the number of FTS active sites to some extent. As stated previously, the iron carbide content of FeSi catalyst did not change significantly during the whole reaction period, thus no obvious change of the CO conversion level was observed [13]. Zr2-A catalyst exhibited the similar reaction behavior in comparison to FeSi catalyst, since the iron carbide content of these two catalysts was almost identical (both in the reduced and used catalysts). This was possibly caused by the fact that the Fe–SiO_2 interaction was not effectively modified by ZrO_2 in Zr2-A catalyst. The weakened Fe–SiO_2 interaction lead to the increased iron carbide content in Zr2-B catalyst, as a result, the activity of Zr2-B catalyst increased relative to that of FeSi catalyst. For Zr2-C catalyst, the highest iron carbide content in the reduced catalyst accounted for its highest initial activity, since no effective Fe–O–Si structure was formed in this sample. However, the iron carbide was gradually oxidized during reaction (evidenced by its lowest iron carbide content in the used catalyst), resulting in the deactivation of this catalyst eventually. Note that ZrO_2 is not a chemical promoter like K, then the difference of the

Table 7
Activity and selectivity of the zirconia-promoted FeSi catalysts.[a,b]

Catalysts	FeSi		Zr2-A		Zr2-B		Zr2-C	
TOS	72	145	72	144	72	144	72	144
CO conversion (%)	63.5	63.2	65.4	69.7	71.9	76.7	81.3	76.3
$CO+H_2$ conversion (%)	51.7	51.7	54.5	58.5	56.9	61.9	64.1	60.4
Exit molar H_2/CO ratio	2.9	2.9	3.1	3.2	3.2	3.8	4.7	3.9
H_2/CO molar usage	1.4	1.4	1.4	1.4	1.3	1.3	1.3	1.3
CO_2 selectivity (mol%)	25.8	26.0	26.7	27.2	25.8	27.3	30.1	30.0
$K_p((PCO_2 \cdot PH_2)/(PCO \cdot PH_2O)$	1.6	1.6	1.9	2.1	1.9	2.4	3.7	2.8
Selectivity (wt%)								
C_1	20.0	22.9	19.9	20.8	22.0	25.3	25.4	27.2
$C_2–C_4$	42.5	43.3	41.0	41.9	42.1	45.6	45.9	48.4
C_5^+	37.5	33.8	39.1	37.3	35.9	29.1	28.7	24.4
$C_2^=–C_4^=/C_2^\circ–C_4^\circ$ (mol/mol)	1.1	1.0	1.2	1.1	0.8	0.7	0.5	0.5
Oxygenates (wt%)[b,c]								
Acid	0.6	0.6	0.5	0.5	0.5	0.5	0.4	0.4
Alcohol	8.9	8.6	9.0	8.9	9.1	9.0	9.5	9.1

[a] Reaction condition: 270 °C, 1.5 MPa, $H_2/CO = 2.0$ and GHSV = 2000 h^{-1}.
[b] Max error = ±3%.
[c] Oxygenates in total CH and oxygenates.

reaction behavior between FeSi and Zr2-B (also Zr2-C) illustrated in Fig. 7 was significant.

3.6.2. Product selectivity

Hydrocarbon product distribution of the catalysts is shown in Table 7. One may find that the methane selectivity was relatively high (20%), this was acceptable since no K promoter was introduced in the present study. For Zr2-A catalyst, the selectivity to gaseous and light hydrocarbons (methane and $C_2–C_4$) were suppressed, whereas those to heavy hydrocarbons (C_5^+) and olefins ($C_2^=–C_4^=/C_2^\circ–C_4^\circ$) were enhanced, when compared to that of FeSi catalyst. However, the selectivity variation of Zr2-B and Zr2-C catalysts exhibited the opposite trend. It is generally accepted that, at least for iron-based FTS catalysts, the surface H/C ratio is a crucial factor in determining the catalysts products distribution [37,38]. The H_2-TPD results indicated that the content of reactive H species (H_α) on the Zr2-B and Zr2-C catalysts surface were higher (in comparison to FeSi catalyst). Therefore a higher surface H/C ratio was expected for these two catalysts. The increased H/C ratio inhibited the chain propagation reaction while enhanced the hydrogenation ability, lowering the selectivity to heavy hydrocarbons and olefins for Zr2-B and Zr2-C catalysts. If one accepts the above statement, then the selectivity variation trend of Zr2-A catalyst was understandable, since the H species on this catalyst surface was more stable than that of FeSi catalyst.

4. Conclusions

In this study, ZrO_2-promoted Fe/SiO_2 catalysts with the same composition were prepared using three different methods. Combined methods (FTIR, TPR, TPD, TEM and MES) were applied to investigate the influence of ZrO_2 addition manner on the $Fe–SiO_2$ interaction, and its effect on the physico-chemical properties and FTS performance of the ZrO_2-modified FeSi catalysts were examined and compared as well. We did not examine the effect of ZrO_2 content variation on the modification of $Fe–SiO_2$ interaction here, since it has been extensively studied previously.

The modification of $Fe–SiO_2$ interaction by ZrO_2 depended strongly on the preparation method of the catalysts. This interaction in Zr2-A catalyst was almost undisturbed. Therefore, no marked difference of the properties (BET surface area, reduction and carburization ability, FTS reaction behavior) between Zr2-A and FeSi (non-promoted) catalysts was observed. For Zr2-B catalyst, however, part of SiO_2 did not interact with iron oxides, which weakened the total strength of $Fe–SiO_2$ interaction to some extent. This enhanced the reduction and carburization ability of Zr2-B catalyst, and increased the FTS reaction activity eventually. It was found that no effective $Fe–SiO_2$ interaction was formed in Zr2-C catalyst, implying that the strong dispersion effect of SiO_2 matrix was greatly destroyed. Consequently, the BET surface area of Zr2-C catalyst decreased obviously. Moreover, higher reduction and carburization degree was observed, which guaranteed the higher initial activity of this catalyst. Whereas the activity was decreased gradually with TOS, this was possibly due to the oxidation of iron carbides, since no obvious $Fe–SiO_2$ interaction formed.

We believe that the present together with the previous study could help to understand the nature of $Fe–SiO_2$ interaction and how ZrO_2 modify this systematically.

Acknowledgements

We thank the National Outstanding Young Scientists Foundation of China (20625620) and the 973 Project from the Ministry of Science and Technology of China (Grant No. 2011CB201401). This work is also supported by Synfuels CHINA. Co., Ltd.

Appendix A. Supplementary data

Supplementary data associated with this article can be found, in the online version, at doi:10.1016/j.cattod.2011.10.024.

References

[1] Y. Traa, Chem. Commun. 46 (2010) 2175.
[2] M. Höök, K. Aleklett, Int. J. Energy Res. 34 (2010) 848.
[3] B.H. Davis, Catal. Today 84 (2003) 83.
[4] E.d. Smit, B.M. Weckhuysen, Chem. Soc. Rev. 37 (2008) 2758.
[5] E. de Smit, F.M.F. de Groot, R. Blume, M. Havecker, A. Knop-Gericke, B.M. Weckhuysen, Phys. Chem. Chem. Phys. 12 (2010) 667.
[6] H. Wang, Y. Yang, J. Xu, H. Wang, M. Ding, Y. Li, J. Mol. Catal. A: Chem. 326 (2010) 29.
[7] W. Ma, E.L. Kugler, D.B. Dadyburjor, Energy Fuels 21 (2007) 1832.
[8] Y. Yang, H.W. Xiang, Y.Y. Xu, L. Bai, Y.W. Li, Appl. Catal. A: Gen. 266 (2004) 181.
[9] D.B. Bukur, C. Sivaraj, Appl. Catal. A: Gen. 231 (2002) 201.
[10] C.H. Zhang, H.J. Wan, Y. Yang, H.W. Xiang, Y.W. Li, Catal. Commun. 7 (2006) 733.
[11] Y. Yang, H.W. Xiang, L. Tian, H. Wang, C.H. Zhang, Z.C. Tao, Y.Y. Xu, B. Zhong, Y.W. Li, Appl. Catal. A: Gen. 284 (2005) 105.
[12] A.F.H. Wielers, A.J.H.M. Kock, C.E.C.A. Hop, J.W. Geus, A.M. van Der Kraan, J. Catal. 117 (1989) 1.
[13] M. Qing, Y. Yang, B. Wu, J. Xu, C. Zhang, P. Gao, Y. Li, J. Catal. 279 (2011) 111.
[14] F.J. Perez-Alonso, M.L. Granados, M. Ojeda, T. Herranz, S. Rojas, P. Terreros, J.L.G. Fierro, M. Gracia, J.R. Gancedo, J. Phys. Chem. B 110 (2006) 23870.
[15] A. Feller, M. Claeys, E.v. Steen, J. Catal. 185 (1999) 120.
[16] S. Bruni, F. Cariati, M. Casu, A. Lai, A. Musinu, G. Piccaluga, S. Solinas, Nanostruct. Mater. 11 (1999) 573.

[17] D. Scarano, A. Zecchina, S. Bordiga, F. Geobaldo, G. Spoto, J. Chem. Soc., Faraday Trans. 89 (1993) 4123.
[18] R. Szostak, V. Nair, T.L. Thomas, J. Chem. Soc., Faraday Trans. 83 (1987) 487.
[19] U. Schwertmann, H. Thalmann, Clay Miner. 11 (1976) 189.
[20] Y. Wang, A. Muramatsu, T. Sugimoto, Colloids Surf. A: Physicochem. Eng. Aspects 134 (1998) 281.
[21] M. Gotic, S. Music, J. Mol. Struct. 834–836 (2007) 445.
[22] S. Ali, B. Chen, J.G. Goodwin, J. Catal. 157 (1995) 35.
[23] H.J. Wan, B.S. Wu, C.H. Zhang, H.W. Xiang, Y.W. Li, B.F. Xu, F. Yi, Catal. Commun. 8 (2007) 1538.
[24] C.R.F. Lund, J.A. Dumesic, J. Catal. 72 (1981) 21.
[25] C.R.F. Lund, J.A. Dumesic, J. Catal. 76 (1982) 93.
[26] C.R.F. Lund, J.A. Dumesic, J. Phys. Chem. 86 (2002) 130.
[27] R. Zboril, M. Mashlan, D. Petridis, Chem. Mater. 14 (2002) 969.
[28] Y. Okamoto, T. Kubota, Y. Ohto, S. Nasu, J. Phys. Chem. B 104 (2000) 8462.
[29] W. Kundig, H. Bommel, G. Constaba, Rh Lindqui, Phys. Rev. 142 (1966) 327.
[30] Am Vanderkr, Phys. Stat. Sol. A 18 (1973) 215.
[31] B. Kolk, A. Albers, I.R. Leith, M.G. Howden, Appl. Catal. 37 (1988) 57.
[32] H. Dlamini, T. Motjope, G. Joorst, G.t. Stege, M. Mdleleni1, Catal. Lett. 78 (2002) 201.
[33] M. Boudart, A. Delbouille, J.A. Dumesic, S. Khammouma, H. Topsøøe, J. Catal. 37 (1975) 486.
[34] E.S. Lox, G.B. Marin, E. De Grave, P. Bussièère, Appl. Catal. 40 (1988) 197.
[35] J.B. Butt, Catal. Lett. 7 (1991) 61.
[36] N. Sirimanothan, H.H. Hamdeh, Y.Q. Zhang, B.H. Davis, Catal. Lett. 82 (2002) 181.
[37] X.H. Mo, J. Gao, N. Umnajkaseam, J.G. Goodwin, J. Catal. 267 (2009) 167.
[38] C. Zhang, G. Zhao, K. Liu, Y. Yang, H. Xiang, Y. Li, J. Mol. Catal. A: Chem. 328 (2010) 35.
[39] G.B. Raupp, W.N. Delgass, J. Catal. 58 (1979) 348.
[40] J.B. Butt, Catal. Lett. 7 (1991) 83.
[41] C.N. Satterfield, R.T. Hanlon, S.E. Tung, Z.M. Zou, G.C. Papaefthymiou, Ind. Eng. Chem. Prod. Res. Dev. 25 (1988) 401.